

The following procedure is recommended for analysis of process β : (1) Define a region AB on the Dalitz plot where the resonance A may distort the analysis. (2) Check that AB does not include any point corresponding to $\cos\lambda_{23}^* = 0$ [see Fig. 1(c)]. (3) Define a C region large enough to contain the $A'B'$ region. (4) For each event included in C , go to the c.m.s. of particles 2 and 3, interchange their direction, and make thereby a fictitious conjugate event. (5) Ignore the fictitious conjugate events which do not fall into AB . (6) Remove the true events from region AB and repopulate this region with the fictitious conjugate events.

One should remember when making the χ^2 fits that the sample of fictitious events is highly correlated statistically to the sample of true events from which the former were constructed.

The same method can be applied to study the process α provided that AB does not include the points where $\cos\lambda_{12}^* = 0$ in the A c.m.s.

Finally, if one makes an analysis of what is in AB region alone and subtracts from the histograms the contributions of β and α , represented by the two kinds of fictitious events in the B c.m.s. and

in the A c.m.s., respectively, one can then study the interference (i.e., process γ) by itself. One should remember, however, that in such an operation, one has subtracted the background (process δ) twice.

An alternate technique to the one proposed above would be to use a rotation, in the c.m.s. of the resonance being studied, of 180° around the normal \hat{n} to the plane of production (instead of the spatial parity operation used above). This is equivalent to the product of a spatial parity operation and a reflection with respect to the production plane (a good operation if over-all parity is conserved). With that alternate technique, one should remember that the conjugation inverts the components of the decay particle spins in the plane of production.

¹Two tests to check the uniformity of the background from process δ are (1) symmetry in $\cos\lambda_{23}^*$ for those events in band B but not in AB or $A'B'$, (2) symmetry with respect to the quantity $(\hat{n} \times \hat{p}_B) \cdot \hat{p}_3^*$ (i.e., left-right symmetry about the direction of B) using the same sample of events as in test (1).

ISOBAR MODEL ANALYSIS OF SINGLE PION PRODUCTION IN PION-NUCLEON COLLISIONS BELOW 1 BeV[†]

M. Olsson* and G. B. Yodh

Department of Physics and Astronomy, University of Maryland, College Park, Maryland

(Received 11 March 1963)

In this paper we show that an improved (3, 3) isobar model for single pion production in pion-nucleon collisions can account for the majority of the observed mass spectra and the ratio of π^0 to π^+ production in $\pi^+ - p$ collisions from 350 MeV to 1 BeV. This is in contrast to earlier analyses using the isobar model.¹⁻⁴ The essential new feature of the present analysis is the inclusion of the P -wave decay of the (3, 3) isobar.

Although the rough features of the shape of the mass spectra predicted by the isobar model of Lindenbaum and Sternheimer¹⁻³ (called LS model hereafter) have been observed in many experiments,⁵⁻⁸ the LS model fails to describe the $\pi - \pi$ mass spectra. The main approximations of the LS model are that (a) the interference between the two isobar diagrams (see Fig. 1) can be neglected, (b) the isobar is produced in a S state and (c) the isobar decays isotropically. Bergia, Bonsignori, and Stanghellini⁴ (called BBS model hereafter)

modified the LS model to include the interference between the two isobar diagrams, still, however, making approximations (b) and (c). They show that interference effects modify the results of the LS model greatly.

We have extended the work of Bergia, Bonsignori,

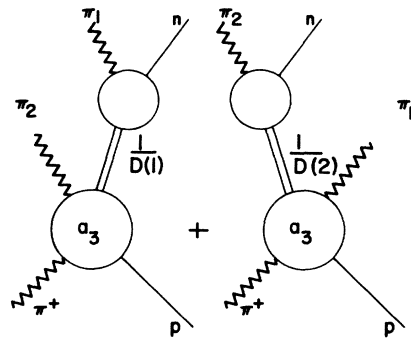


FIG. 1. Two isobar diagrams for the reaction $\pi + p \rightarrow \pi_1 + \pi_2 + N$.

ori, and Stanghellini to include, in addition to the interference between the two diagrams, (1) the P -wave decay of the isobar and (2) requirements of Bose statistics. We still assume S -wave production for the isobar. In this model, the matrix elements for the $\pi^+ - p$ reactions

$$\pi^+ + p \rightarrow \pi^+ + \pi^+ + n \quad (1)$$

and

$$\pi^+ + p \rightarrow \pi^+ + \pi^0 + p \quad (2)$$

are given by

$$M(\pi^+, \pi^+, n) = -\frac{a_2 \vec{\sigma} \cdot \hat{q}}{\sqrt{60}} \left[\frac{S(\hat{p}_2')}{D(2)} + \frac{S(\hat{p}_1')}{D(1)} \right] \quad (3)$$

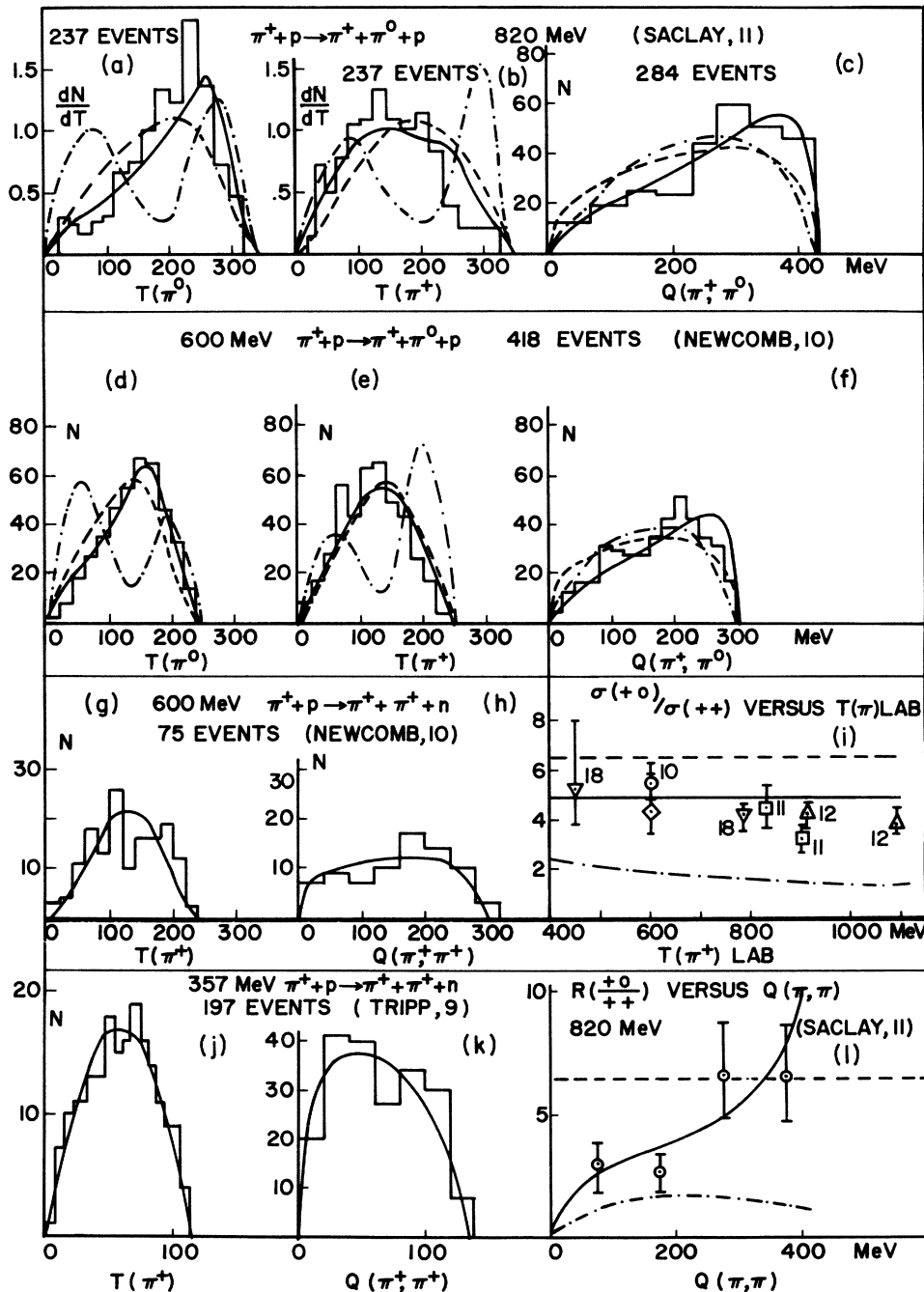


FIG. 2. Comparison of experimental data for Reactions (1) and (2) at 357, 600, and 820 MeV with isobar model predictions. Solid curve is the model described in this paper, dashed curves represent the LS model,¹ and the dot-dashed curves represent the BBS model.⁴ All curves are normalized to total number of events.

and

$$M(\pi^+, \pi^0, p) = \frac{a_3 \vec{\sigma} \cdot \hat{q}}{\sqrt{15}} \left[\frac{3S(\hat{p}_1')}{2D(1)} - \frac{S(\hat{p}_2')}{D(2)} \right]. \quad (4)$$

Here $a_3 \vec{\sigma} \cdot \hat{q}/D(1)$ denotes the $T = \frac{3}{2}$ amplitude for S-wave production of the isobar formed by pion No. 1 and the nucleon [a corresponding definition holds for $a_3 \vec{\sigma} \cdot \hat{q}/D(2)$]. The factor $D(1)$ represents the resonance denominator for the (3, 3) resonance and is given by⁹

$$\frac{1}{D(1)} = \frac{[\Gamma(1)]^{1/2}}{W(1N) - W_R + i\Gamma(1)},$$

where $\Gamma(1)$ is the width, W_R the (3, 3) resonance energy, and $W(1N)$ the energy of pion No. 1 and nucleon in their center of mass [a corresponding formula holds for $1/D(2)$]. The incoming pion direction in the over-all center of mass is given by the unit vector \hat{q} . The P-wave decay of the isobar is given by the function

$$S(\hat{p}_2') = [2\hat{q} \cdot \hat{p}_2' - i\vec{\sigma} \cdot (\hat{q} \times \hat{p}_2')],$$

where \hat{p}_2' is the direction of motion of pion No. 2, which forms the isobar, in the isobar center of mass, and $\vec{\sigma}$ is the nucleon spin. Apart from the

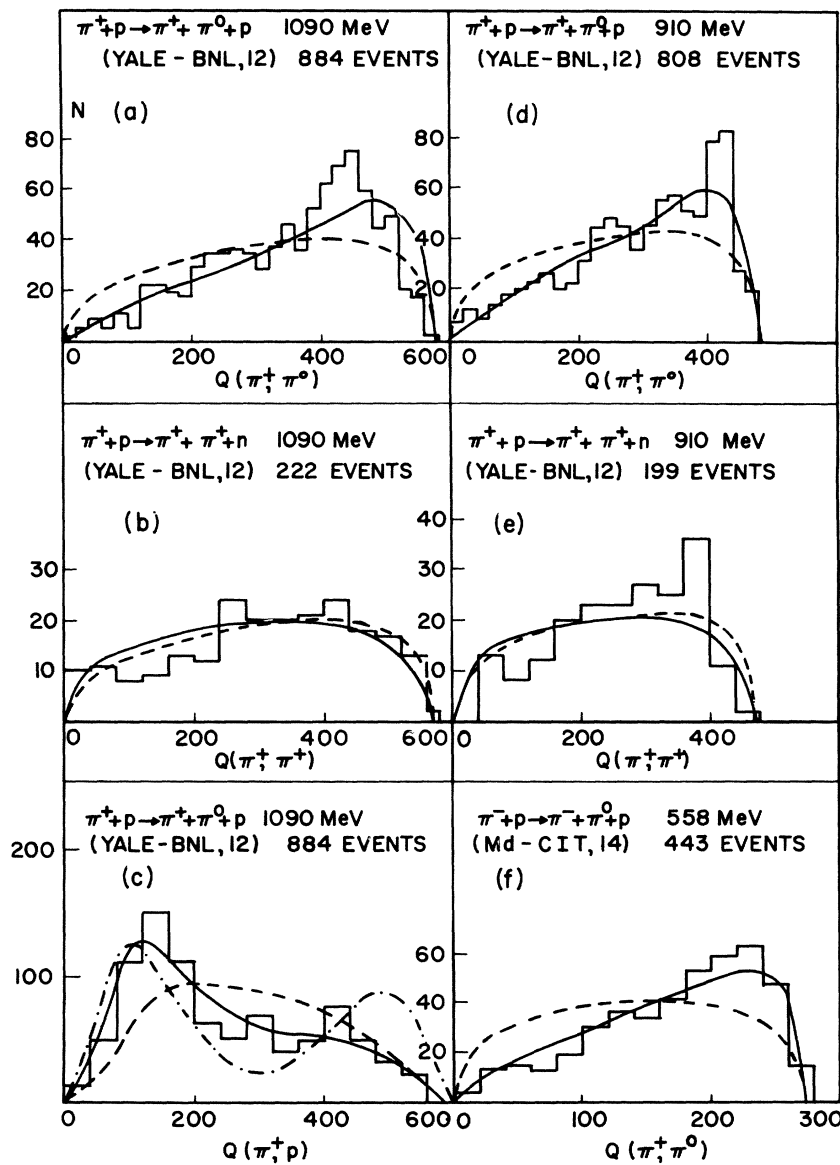


FIG. 3. Comparison of experimental data for Reactions (1) and (2) at 900¹⁴ and 1090¹⁴ MeV. The graph on the lower right-hand corner is for the reaction $\pi^- + p \rightarrow \pi^- + \pi^0 + p$ at 558 MeV.¹⁴

over-all factor a_3 , which could be energy dependent, there are no free parameters in these matrix elements. The matrix elements for the corresponding charged inelastic π^-p reactions involve two parameters, the ratio of the magnitudes of amplitudes for pion production in $T = \frac{3}{2}$ and $T = \frac{1}{2}$ states, and their phase difference.¹⁰

Next, we compare the predictions of our model with data on Reactions (1) and (2) at 357,¹¹ 600,¹² 820,¹³ 910,¹⁴ and 1090¹⁴ MeV and $\pi^- - p$ reactions at 558 MeV.¹⁵

(i) The ratio of π^0 to π^+ production as a function of the laboratory kinetic energy of the pion is compared with the LS model and the present model in Fig. 2 (i). The LS model predicts a constant ratio of 6.5, while our model gives a slowly decreasing ratio of about 5, which is in reasonable agreement with data. The BBS model gives a ratio varying from 2.5 to 1.2.

(ii) The shape of the mass spectra for Reactions (1) and (2) are compared with the predictions of the present model, the LS model, and the BBS model in Figs. 2 and 3. The projection of the folded Dalitz plots and the $Q(\pi^+, \pi^+)$ spectra for Reaction (1), at 357, 600, 910, and 1090 MeV, are in good agreement with the present model as well as the LS model. For Reaction (2), the present model accounts for the shape of all three projections of the Dalitz plot [$T(\pi^+)$, $T(\pi^0)$, and $Q(\pi^+, \pi^0)$], in contrast to other models. The BBS model, in fact, leads to a pronounced interference dip in the $T(\pi^+)$ and $T(\pi^0)$ spectra. The depletion for small $Q(\pi^+, \pi^0)$ and the enhancement for large $Q(\pi^+, \pi^0)$ follows from the nature of Eq. (4). As the matrix element is almost antisymmetric in the exchange of the two pions, it is small in the region where the vector momenta of the two pions are equal, while in the region where the momenta are equal and opposite it is large.

(iii) Figure 2(l) shows the ratio of π^0 to π^+ events as a function of $Q(\pi, \pi)$ at 820 MeV.¹³ Here the agreement with our model is striking. The low value for the ratio for small $Q(\pi, \pi)$ is a consequence of the antisymmetry in Eq. (4) and the symmetry in Eq. (3). The LS model would predict a constant value of 6.5, while the BBS model gives a value varying from 0.25 to 1.5.

(iv) In the $Q(\pi^+, \pi^0)$ spectra at 910 and 1090 MeV, the ρ meson is beginning to appear near the upper end. It is clear that the presence of a strong (3, 3) isobar makes it very difficult to estimate ρ production quantitatively. The shape of the $Q(\pi^+, \pi^0)$ curve calculated from this model is quite similar to one which would be obtained from OPE

diagram assuming a constant $\pi - \pi$ cross section.¹⁴

(v) We have compared the $Q(\pi^+, \pi^0)$ curves at 820,¹³ 900,¹³ 910,¹⁴ 1050,¹³ and 1090¹⁴ MeV with our model. We find no statistically significant evidence for the reported ξ meson of mass 575 MeV.

(vi) The shape of the $Q(\pi^-, \pi^0)$ spectra in the reaction $\pi^- + p \rightarrow \pi^- + \pi^0 + p$, at 558¹⁵ MeV is shown in Fig. 3(f), and one sees that the LS model gives no agreement with data while the present model agrees well with observed distribution. Good agreement of our model with $Q(\pi^-, \pi^0)$ spectra at 604 MeV¹⁶ is also obtained.

(vii) Only in the reaction $\pi^- + p \rightarrow \pi^- + \pi^+ + n$ does the present model fail to describe the shape of the $Q(\pi^-, \pi^+)$ spectra,¹⁷ in particular, the peaking near maximum Q values. This would indicate that there could be some two-pion interaction in isotopic spin-zero state which modifies the simple isobar model. However, the importance of the (3, 3) isobar in this reaction is clearly indicated in the pion-nucleon mass spectra in the region below 1 BeV.¹⁸ We are investigating the influence of such $\pi - \pi$ interactions and other nonresonant background on mass spectra and angular distributions.

We wish to thank Dr. J. Sucher, Dr. R. Karplus, Dr. O. W. Greenberg, Dr. T. B. Day, and Dr. G. A. Snow for many discussions, and Dr. Peter Newcomb for allowing us to use his data. Dr. Day's help in running on the computer is gratefully acknowledged.

[†]Work done under the auspices of the U. S. Atomic Energy Commission.

*National Science Foundation Predoctoral Fellow.

¹S. J. Lindenbaum and R. M. Sternheimer, Phys. Rev. **105**, 1874 (1957).

²S. J. Lindenbaum and R. M. Sternheimer, Phys. Rev. **106**, 1107 (1957).

³R. M. Sternheimer and S. J. Lindenbaum, Phys. Rev. **109**, 1723 (1958).

⁴S. Bergia, F. Bonsignori, and A. Stanghellini, Nuovo Cimento **15**, 1073 (1960).

⁵W. D. Walker, F. Hushfar, and W. D. Shepard, Phys. Rev. **104**, 526 (1956).

⁶A. P. Batson, B. B. Culwick, J. G. Hill, and L. Riddiford, Proc. Roy. Soc. (London) **A251**, 218 (1959).

⁷G. B. Chadwick, G. B. Collins, C. E. Swartz, A. Roberts, S. DeBenedetti, N. C. Hien, and P. J. Duke, Phys. Rev. Letters **4**, 611 (1960).

⁸V. Alles-Borelli, S. Bergia, E. Perez Ferreira, and P. Waloschek, Nuovo Cimento **14**, 211 (1959).

⁹H. A. Bethe and F. de Hoffman, Mesons and Fields

(Row, Peterson and Company, Evanston, 1955), Vol. II, p. 131.

¹⁰In the notation of reference 3 we have determined the parameters to be $\rho = 0.13$ and $\phi = 120^\circ$.

¹¹Janos Kirz, Joseph Schwartz, and Robert D. Tripp, Bull. Am. Phys. Soc. 7, 48 (1962); Phys. Rev. 126, 763 (1962).

¹²P. Newcomb, Bull. Am. Phys. Soc. 7, 468 (1962); Lawrence Radiation Laboratory Report UCRL-10682, 1963 (unpublished). New data at 600 MeV from Saclay [Nuovo Cimento 26, 1409 (1962)] give very similar results. Their value of the $(+0)/(++) = 4.5 \pm 1.1$ is plotted in Fig. 2.

¹³R. Barloutand, J. Heughebaert, A. Leveque, J. Mey-

er, and R. Omnes, Phys. Rev. Letters 8, 32 (1962).

¹⁴D. L. Stonehill and H. L. Kraybill, Rev. Modern Phys. 34, 503 (1962).

¹⁵G. B. Yodh, T. B. Day, G. Quareni, A. Quareni-Vignudelli, R. A. Burnstein, J. Ashkin, I. Nadelhaft, and J. Oliver, Bull. Am. Phys. Soc. 8, 68 (1963).

¹⁶C. N. Vittetoe, W. J. Fickinger, V. P. Kenney, J. G. Mowat, and W. D. Shepard, Bull. Am. Phys. Soc. 8, 67 (1963).

¹⁷J. Kirz, J. Schwartz, and R. D. Tripp, Bull. Am. Phys. Soc. 8, 68 (1963); Lawrence Radiation Laboratory Report UCRL-10676, 1963 (unpublished).

¹⁸C. P. Poirer, E. D. Alyea, H. J. Martin, and C. A. Tilger, Bull. Am. Phys. Soc. 8, 68 (1963).

THEORY OF SCATTERING WITH LARGE MOMENTUM TRANSFER

Robert Serber*

Columbia University, New York, New York

(Received 21 March 1963)

It is surprising that it has not previously been observed that the measurements of the elastic proton-proton scattering for high momentum transfers follow a simple power law. This is shown by Fig. 1, in which all the experimental results of the CERN and Brookhaven groups,¹ for proton initial momentum greater than 8 BeV/c, are shown on a log-log plot as a function of the square of the momentum transfer, t . A relationship

$$(4\pi/k\sigma_{\text{tot}})^2 d\sigma/d\Omega = \text{const}/t^5 \quad (1)$$

is seen to hold over a range of five decades. Here k is the wave number of the particle being scattered, $d\sigma/d\Omega$ is the differential elastic cross section, and σ_{tot} is the total cross section.

We shall show that this empirical law can be understood in terms of an optical model in which the medium is taken to be purely absorptive, and to be spatially distributed according to a Yukawa function. Thus the change in wave number in the scattering region is

$$k' - k = i\eta e^{-\Lambda r}/r. \quad (2)$$

The optical model gives for the scattering amplitude²

$$f(\theta) = ik \int_0^\infty [1 - e^{2i\delta(\rho)}] J_0(k\theta\rho) \rho d\rho, \quad (3)$$

and for the total and elastic cross sections

$$\sigma_{\text{tot}} = 4\pi \int_0^\infty [1 - e^{2i\delta(\rho)}] \rho d\rho, \quad (4)$$

$$\sigma_{\text{el}} = 2\pi \int_0^\infty [1 - e^{2i\delta(\rho)}]^2 \rho d\rho, \quad (5)$$

and the phase shift is

$$2\delta(\rho) = \int_{-\infty}^\infty (k' - k) ds, \quad (6)$$

with $r^2 = s^2 + \rho^2$. From (6) and (2) we find $\delta(\rho) = i\eta K_0(\Lambda\rho)$.

If we measure the momentum transfer in units of Λ , $y = k\theta/\Lambda$, Eqs. (3), (4), and (5) take the form

$$f(\theta) = i(k/\Lambda^2)F(\eta, y^2), \quad (7)$$

$$\sigma_{\text{tot}} = (4\pi/\Lambda^2)S(\eta), \quad (8)$$

$$\sigma_{\text{el}} = (2\pi/\Lambda^2)s(\eta), \quad (9)$$

with

$$F(\eta, y^2) = \int_0^\infty \{1 - \exp[-2\eta K_0(x)]\} J_0(yx) x dx, \quad (10)$$

$$S(\eta) = F(\eta, 0) = \int_0^\infty \{1 - \exp[-2\eta K_0(x)]\} x dx, \quad (11)$$

$$s(\eta) = \int_0^\infty \{1 - \exp[-2\eta K_0(x)]\}^2 x dx. \quad (12)$$

In Table I we give some values of $S(\eta)$ and $s(\eta)$, and in Fig. 2 we have plotted $(\Lambda^2/4\pi)\sigma_{\text{tot}} = S(\eta)$ and $(\sigma_{\text{el}}/\sigma_{\text{tot}}) = s(\eta)/2S(\eta)$ as functions of η .

Eq. (10) for $F(\eta, y^2)$ is convenient for small y ; to find a form good for large y , write $J_0(yx) = \frac{1}{2} \times [H_0^{(1)}(yx) + H_0^{(2)}(yx)]$ and rotate the two resulting integrals to the positive and negative imaginary